NASA TECHNICAL NOTE

NASA TN D-5809

C.1

NASA TN D-5809



# UNSTABLE BUBBLE MOTION UNDER LOW GRAVITATIONAL CONDITIONS

*by John B. Haggard, Jr.*

*Lewis Research Center*

*Cleveland, Ohio* 44135

NATIONAL AERONAUTICS AND SPACE ADMINISTRATION • WASHINGTON, D. C. • MAY 1970

| | | |
|---|---|---|
| 1. Report No. NASA TN D-5809 | 2. Government Accession No. | 3. Recipient's Catalog No. |
| 4. Title and Subtitle UNSTABLE BUBBLE MOTION UNDER LOW GRAVITATIONAL CONDITIONS | | 5. Report Date May 1970 |
| | | 6. Performing Organization Code |
| 7. Author(s) John B. Haggard, Jr. | | 8. Performing Organization Report No. E-5537 |
| 9. Performing Organization Name and Address Lewis Research Center National Aeronautics and Space Administration Cleveland, Ohio 44135 | | 10. Work Unit No. 124-08 |
| | | 11. Contract or Grant No. |
| 12. Sponsoring Agency Name and Address National Aeronautics and Space Administration Washington, D.C. 20546 | | 13. Type of Report and Period Covered Technical Note |
| | | 14. Sponsoring Agency Code |
| 15. Supplementary Notes | | |

16. Abstract

An experimental study was conducted to examine some fundamental aspects of the motion of single noncondensable bubbles under low gravitational conditions. An acceptable criterion was found for predicting the onset of unstable bubble motion which was consistent with published stability calculations at normal gravity. Data are also presented on the changes of frequency and amplitude of unstable (oscillatory) motion that occur in low gravity. The findings are applicable to bubbles in low-viscosity isothermal fluids at both normal and reduced gravity.

| | |
|---|---|
| 17. Key Words (Suggested by Author(s)) Bubbles Low gravity Weightlessness Two-phase flow | 18. Distribution Statement Unclassified - unlimited |

| | | | |
|---|---|---|---|
| 19. Security Classif. (of this report) | 20. Security Classif. (of this page) | 21. No. of Pages | 22. Price * |
| Unclassified | Unclassified | 19 | $3.00 |

*For sale by the Clearinghouse for Federal Scientific and Technical Information
Springfield, Virginia 22151

# UNSTABLE BUBBLE MOTION UNDER LOW GRAVITATIONAL CONDITIONS

by John B. Haggard, Jr.

Lewis Research Center

## SUMMARY

An experimental study was conducted to examine some fundamental aspects of the nonrectilinear motion of single noncondensable bubbles under low gravitational conditions. An acceptable criterion was found for predicting the onset of unstable bubble motion which was consistent with published stability calculations at normal gravity. Data are also presented on the changes of frequency and amplitude of unstable (oscillatory) motion that occur in low gravity. The findings are applicable to bubbles in low-viscosity isothermal fluids at both normal and reduced gravity.

## INTRODUCTION

Understanding and predicting the motion of bubbles in low-viscosity fluids is of considerable importance in designing liquid-vapor systems aboard space vehicles. Both pump cavitation and costly liquid venting may result if the clusters of bubbles that may exist in tanks aboard spacecraft in low gravity are not properly taken into account. Predicting the motion of single bubbles is part of the knowledge needed to understand the motion of clusters of bubbles. Two important aspects of the dynamics of bubble motion are the terminal velocity and the path of the bubble. In normal gravity, bubbles move in rectilinear paths when they are spherical and have Reynolds numbers less than several hundred. For higher Reynolds numbers, bubbles are distorted and move in helical or zig-zag paths, that is, with unstable motion.

In low gravity, Haggard and Masica (ref. 1) correlated the terminal velocity and shape of single bubbles moving in rectilinear paths as a function of the system acceleration and liquid properties. This report is concerned with establishing a criterion for predicting the onset of unstable motion in low gravity. Knowledge of the path a bubble takes through the liquid, whether rectilinear or unsteady, can be helpful in determining the rates of coalescence and the mutual effect one bubble has on its neighbors.

A search of the literature for work done on low-gravity unstable single bubble motion revealed no reports. For work done in normal gravity, two reports of interest were found. Saffman (ref. 2) examined zig-zag motion and arrived at a value of 1.03 for the critical Weber number (based on bubble radius), that is, the Weber number above which bubble motion is unstable and below which it is stable. He also analyzed the terminal velocity of bubbles with helical motion in water by assuming inviscid flow at the front of the bubbles and examining the pressure distribution over the front surface. Hartunian and Sears (ref. 3) theoretically and experimentally investigated the motion of a deformable sphere moving at a constant velocity in an inviscid fluid at various Weber numbers. Their results led to unstable bubble motions above a certain Weber number (3.18). This indicated to them that the surface tension - hydrodynamic pressure interaction could yield unsteady motion. Their experiments on many test liquids tended to confirm their analysis.

This report presents the results of an experimental study in low gravity to determine when unsteady bubble motion would occur. Measurements of the frequency and amplitude of oscillation after the onset of unstable motion are presented. The results are compared with normal-gravity data. The study was conducted in the Lewis Research Center's Zero-Gravity Facility, where gravity levels from 0.03 to 0.05 g were attained. Bubble radii ranged from 0.17 to 0.87 centimeter.

## SYMBOLS

| | |
|---|---|
| $A$ | amplitude of unstable oscillation of bubble, cm |
| $A_x$ | amplitude of oscillation in x direction, cm |
| $A_y$ | amplitude of oscillation in y direction, cm |
| $a$ | acceleration, $cm/sec^2$ |
| $B_o$ | Bond number, $4r_{eq}^2 a/\beta$ |
| $C$ | constant |
| $d_x, d_y, d_z$ | distances along coordinate axes, cm |
| $g$ | acceleration due to gravity, 980 $cm/sec^2$ |
| $K$ | constant |
| $L$ | constant |

| | |
|---|---|
| Re | Reynolds number, $2r_{eq}v/\nu$ |
| $r_{eq}$ | equivalent radius of spherical bubble of same volume as observed bubbles, cm |
| $r_h$ | average semimajor axis perpendicular to direction of motion of bubble, cm |
| $r_z$ | average semiminor axis parallel to direction of motion of bubble, cm |
| t | time, sec |
| v | terminal velocity, cm/sec |
| We | Weber number, $2r_{eq}v^2/\beta$ |
| $\beta$ | specific surface tension, $\sigma/\rho$, $cm^3/sec^2$ |
| $\eta$ | liquid viscosity, cP |
| $\theta$ | angle between plane of zig-zag motion and x-z plane |
| $\nu$ | kinematic viscosity, $\eta/\rho$, $cm^2/sec$ |
| $\rho$ | liquid density, $g/cm^3$ |
| $\sigma$ | surface tension, dynes/cm |
| $\omega$ | frequency of unstable oscillation of bubble, rad/sec |

# APPARATUS AND PROCEDURE

## Test Liquids

The following liquids were used in this study: 1-butanol, methanol, carbon tetrachloride, trichlorotrifluoroethane, and FC-78 (trade name of fluorocarbon solvent made by the 3M Co.). All were analytic reagent grade liquids. Values for the three liquid properties pertinent to this study (density, viscosity, and surface tension), which are given in handbooks and reference 4, are listed in table I. These properties were used in the calculations of the Reynolds number, the Weber number, and the Bond number. The investigation was limited to low-viscosity (0.5 to 3.0 cP) liquids because bubbles in these liquids exhibit greater and more easily observed terminal velocities.

TABLE I. - SUMMARY OF LIQUID PROPERTIES

| Liquid | Density, $\rho$, g/cm$^3$ | Temperature, $^{\circ}C$ | Surface tension, $\sigma$, dynes/cm | Temperature, $^{\circ}C$ | Viscosity, $\eta$, cP | Temperature, $^{\circ}C$ |
|---|---|---|---|---|---|---|
| Methanol | 0.791 | 20 | 24.5 | 0 | 0.60 | 20 |
| | .787 | 25 | 22.6 | 20 | .55 | 25 |
| | .782 | 30 | 20.1 | 50 | .51 | 30 |
| FC-78 | 1.725 | 18 | 13.2 | 20 | 0.82 | 19 |
| | 1.716 | 24 | 12.6 | 25 | .79 | 22 |
| | 1.700 | 30 | 12.3 | 29 | .75 | 25 |
| Carbon tetrachloride | 1.613 | 10 | 28.0 | 10 | 0.97 | 20 |
| | 1.595 | 20 | 26.8 | 20 | .84 | 30 |
| | 1.575 | 30 | 25.5 | 30 | .74 | 40 |
| Trichlorotrifloroethane | 1.579 | 20 | 18.6 | 20 | 0.70 | 20 |
| | 1.565 | 25 | 17.3 | 25 | .68 | 25 |
| | 1.534 | 30 | ---- | -- | ---- | -- |
| 1-Butanol | 0.813 | 15 | 26.2 | 0 | 3.38 | 15 |
| | .810 | 20 | 24.2 | 20 | 2.95 | 20 |
| | .806 | 25 | 22.1 | 50 | 2.30 | 30 |

## Low-Gravity Tests

Test facility. - The experimental tests were conducted in the Zero-Gravity Facility shown in figure 1. The free-fall distance of 24 meters allowed a 2.2-second period of weightlessness. Air drag on the experiment package was reduced to less than $10^{-5}$ g by allowing the experiment package to fall inside a drag shield. During the drop, the package and drag shield fell simultaneously but were independent of each other. The sequential position of the experiment package in the drag shield during the test drop is shown in figure 2. Low gravity was achieved on the experiment package by means of a gas thruster. The package was decelerated by the penetration of the drag shield spikes into the sand of the deceleration container.

Experiment package. - The experiment tank was mounted in the experiment package shown in figure 3. The experiment package contained a high-speed, 16-millimeter, motion picture camera and a uniform backlighting scheme. A digital clock accurate to 0.01 second was in the field of view of the camera. Both the calibration of the thrust, used to apply a low-gravity acceleration, and the alinement of the center of mass of the package through the thrust axis were performed according to the procedure outlined in reference 5.

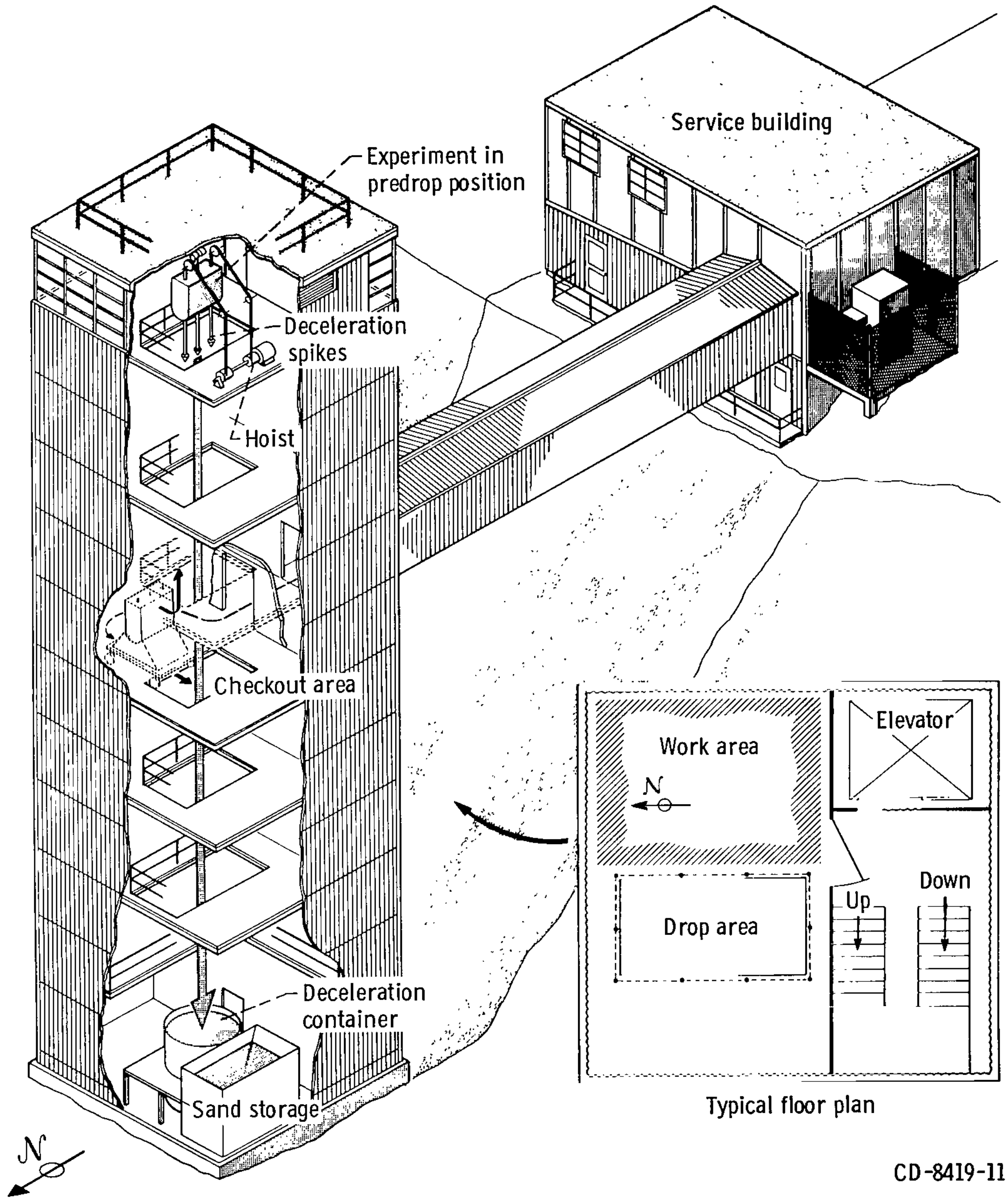


Figure 1. - 2.2-Second zero-gravity facility.

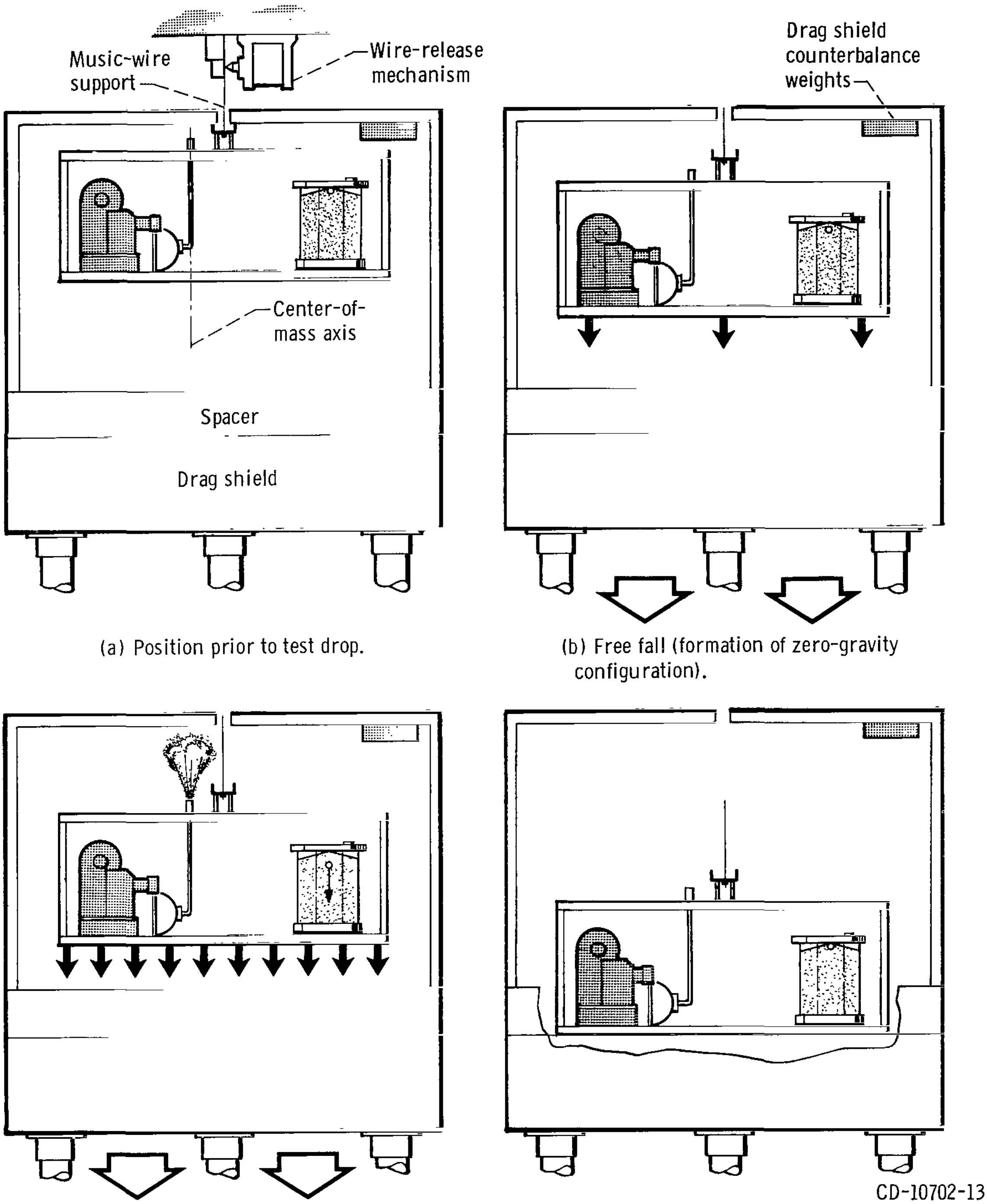


(a) Position prior to test drop.

(b) Free fall (formation of zero-gravity configuration).

(c) Application of thrust (low-acceleration field).

(d) Position after test drop.

Figure 2. - Sequencial position of experiment package and drag shield before, during, and after test drop.

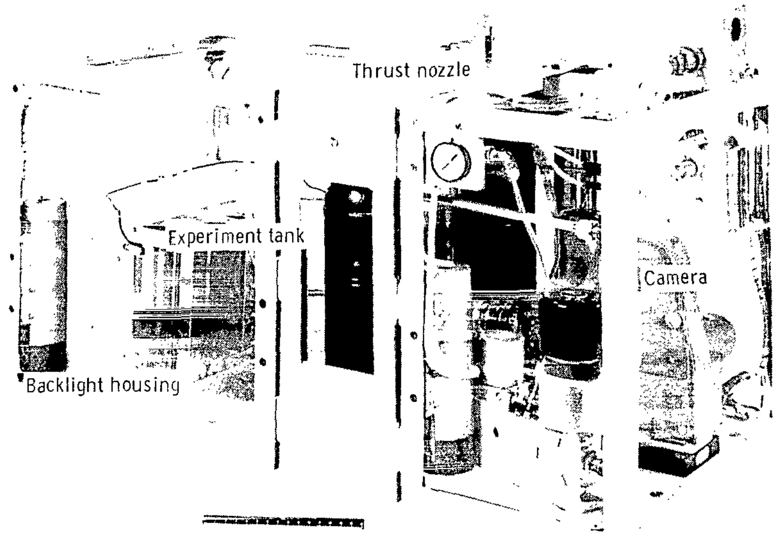


Figure 3. - Experiment package.

Experiment tank. - The acrylic plastic tank (fig. 4) used in low-gravity tests was octagonal. This shape minimized refraction as well as liquid volume. The tank was 19 centimeters high and 13.96 centimeters between faces. Each face was 5.78 centimeters wide. Side mirrors were installed to provide a three-dimensional view of the movement of the bubble. The insert at the top of the tank was designed with an apex in it to provide an initial position for the vapor bubble. The top also contained a reservoir filled with the test liquid and a fill-vent line extending down into the tank. The reservoir provided an expansion volume to prevent either bubble collapse or unwanted vapor from being pulled into the fill-vent lines whenever the liquid expanded or contracted slightly because of ambient temperature changes. The tank used in this study was large enough so that wall effects were negligible. Reference 6 indicated that wall effects are negligible whenever the ratio of tank diameter to bubble diamter is greater than 10. The ratio of tank diameter to bubble diameter for the test runs ranged from 8.0 to 41. Scales with 0.2-centimeter divisions were mounted on two faces of the tank. Appropriate parallax corrections were made when necessary.

Operating procedure. - Before each test, the tank was ultrasonicially cleaned in a mild detergent solution, rinsed in distilled water, rinsed again in pure methanol, and dried in warm filtered air. This procedure was followed to prevent the tank from contaminating the test liquid. The tank was filled with liquid, and a measured amount of air was injected into the tank with a microliter syringe through the fill-vent line. The result-

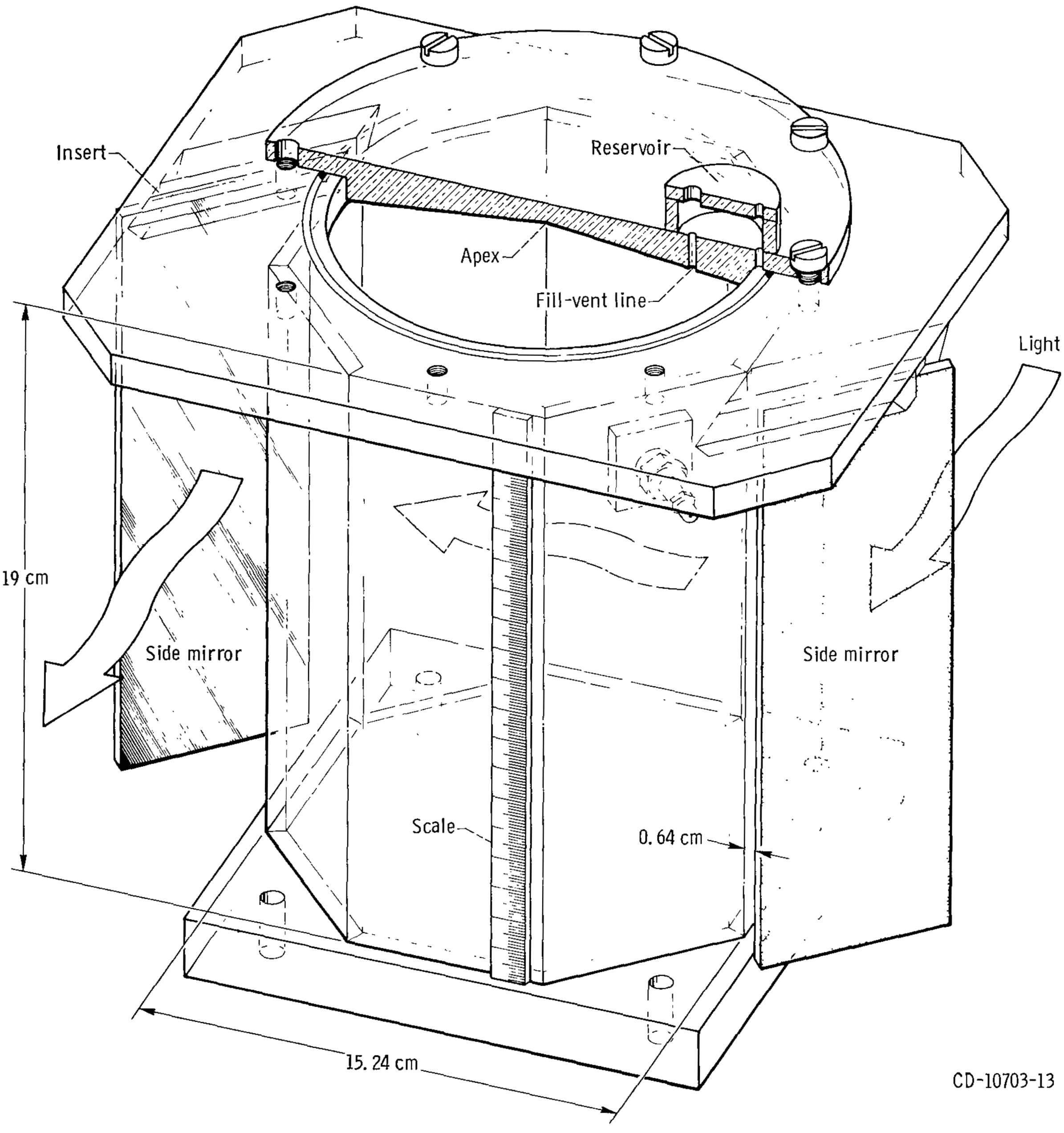


Figure 4. - Experiment tank used in low-gravity tests.

ing bubble was positioned at the apex of the tank. Two seconds before the drop, the camera and lights were turned on. When the experiment package was released, the thruster started and remained on for the balance of the drop. An isothermal condition was assumed for the system during the drop.

## Normal-Gravity Tests

The tank used in normal-gravity tests is shown in figure 5. It had a square cross

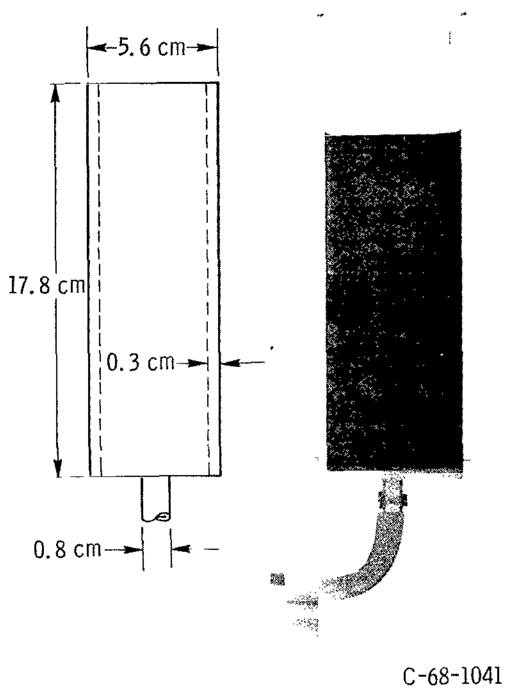


Figure 5. - Experiment tank used in normal-gravity tests.

section 5.6 by 5.6 centimeters and was 17.8 centimeters high. The ratio of tank diameter to bubble diameter ranged from 17 to 80; hence, wall effects were again negligible. Prior to each test, the tank was also ultrasonically cleaned and filled with liquid. With a microliter syringe, a measured amount of air was injected into the tube that extended from the bottom of the tank. The bubble moved along the length of the tube and moved into the tank. As the bubble rose in the tank, it was photographed with a high-speed camera. The liquid temperature was recorded just before the test.

# RESULTS AND DISCUSSION

## Experimental Data

Vertical bubble velocity, bubble size, and path measurements were typicially obtained from the motion picture film of each test during the last second of the drop. The motion of a bubble for a typical low-gravity test is shown in figure 6. In the particular run shown, the test tank was filled with methanol, the acceleration was 49.7 centimeters

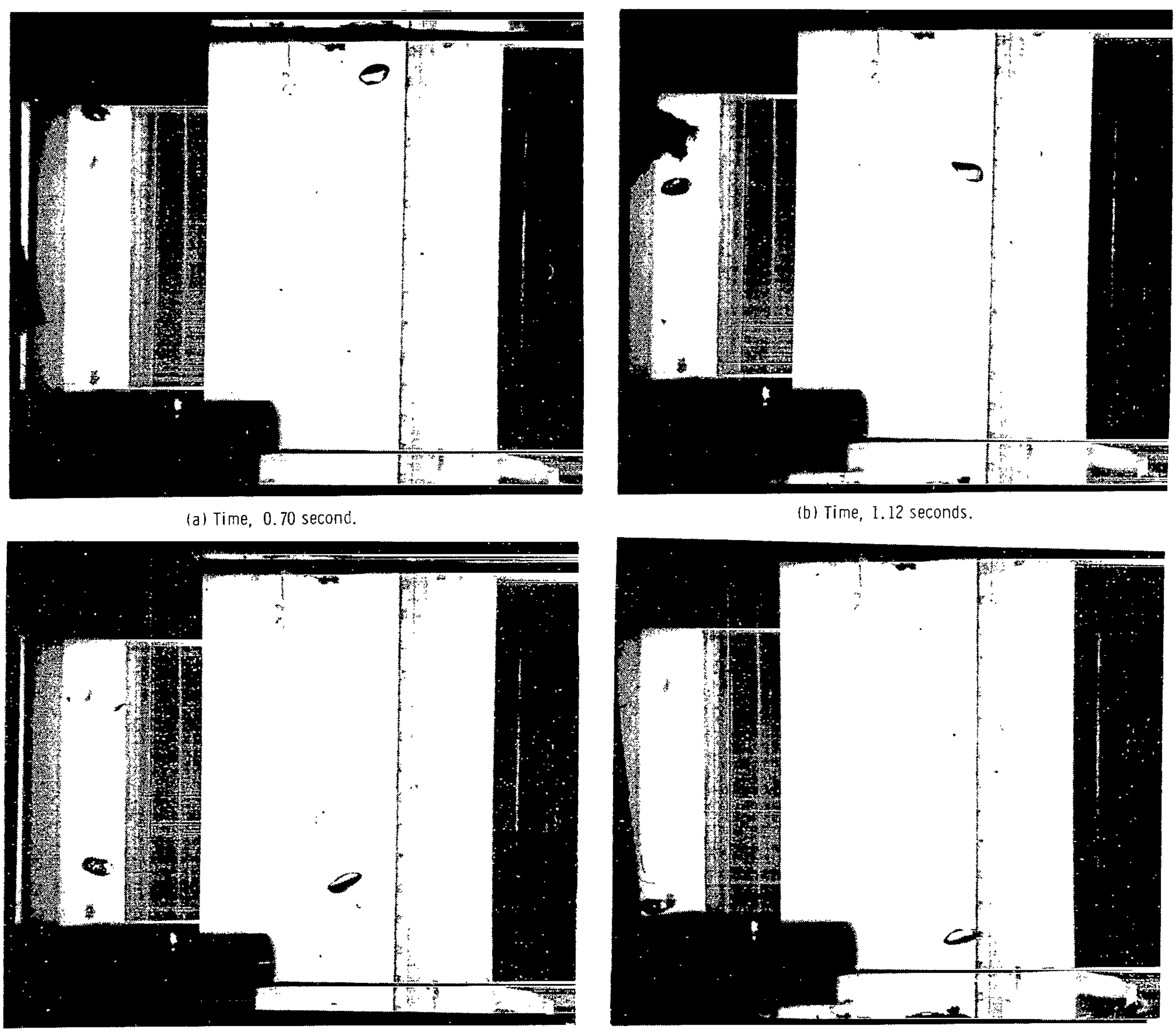

(a) Time, 0.70 second.

(b) Time, 1.12 seconds.

(c) Time, 1.80 seconds.

(d) Time, 2.11 seconds.

Figure 6. - Typical run sequence.

per second squared and the bubble radius was 0.45 centimeter, resulting in a vertical velocity of 9.6 centimeters per second. The bubble, initially at the apex of the tank, was accelerated to its terminal velocity, at which time the bubble exhibited either rectilinear, zig-zag, or helical motion for the remainder of the drop. Zig-zag motion means that the bubble oscillates in a plane that contains the axis of symmetry of the tank as the bubble is traveling at a constant terminal velocity along the direction of this axis of symmetry. Helical motion means that the bubble moves in a spiral on an imagined cylinder having a radius much smaller than the tank radius and that its axis of symmetry coincides with the axis of symmetry of the tank. As with zig-zag motion, the motion in the direction of this axis was constant. It was also observed that, when a bubble in a low-gravity test exhibited zig-zag or helical motion, it also had rather severe rocking motions about its center of mass.

The time and distances the bubble traveled in the x, y, and z directions were measured at intervals throughout the test (see fig. 7). The velocity in the z direction was considered the terminal velocity of the bubble. After the bubble had reached terminal velocity, bubble diameter measurements were taken in each of the three directions. The bubble closely resembled an oblate ellipsoid with the z diameter suppressed. The three

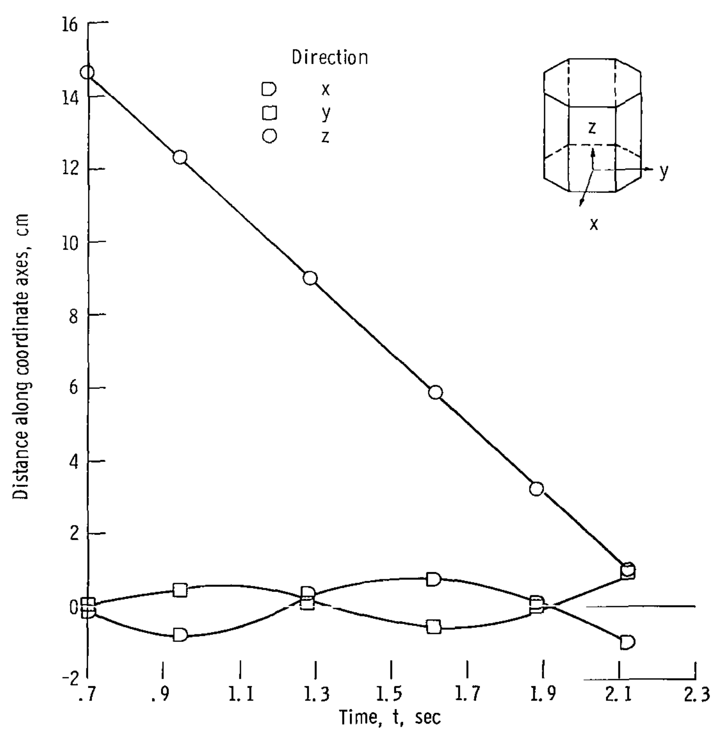

Figure 7. - Position of bubble from typical run.

diameters measured were always the minor and two major axes of the bubble. The equivalent radius of the bubble to a good approximation was given by

$$r_{eq} = \left[r_z\left(r_h\right)^2\right]^{1/3} \tag{1}$$

From the data in figure 7, a determination of the type of bubble motion can be made. For rectilinear motion, the $d_x$ and $d_y$ curves should be zero. For zig-zag motion, the curves follow the relations

$$d_x = A_x \sin \omega t \tag{2a}$$

$$d_y = A_y \sin \omega t \tag{2b}$$

where

$$A_x = A \cos \theta$$

$$A_y = A \sin \theta$$

and for helical motion, the $d_x$ and $d_y$ curves follow the relations

$$d_x = A \sin \omega t \tag{3a}$$

$$d_y = A \cos \omega t \tag{3b}$$

Frequency measurements were calculated from the reciprocal of the time for one cycle in the x or y direction times $2\pi$. The amplitude of oscillation in the case of zig-zag motion was the maximum displacement from the axis. The amplitude was found experimentally for zig-zag motion by the relation

$$A = \left(A_x^2 + A_y^2\right)^{1/2} \tag{4}$$

For helical motion, the amplitude of oscillation was taken to be the radius of the spiral. This amplitude was the average amplitude obtained from the $d_x$ and $d_y$ curves. Once these parameters were collectively determined, the appropriate dimensionless param-

TABLE II. - SUMMARY OF EXPERIMENTAL RESULTS

| Liquid | Acceleration, a, cm/sec$^2$ | Equivalent radius of spherical bubble of same volume as observed bubbles, $r_{eq}$, cm | Terminal velocity, v, cm/sec | Frequency, $\omega$, rad/sec | Amplitude of unstable oscillation of bubble, A, cm | Weber number, We | Bond number, $B_o$ | Reynolds number, Re | Type of motion |
|---|---|---|---|---|---|---|---|---|---|
| Methanol | 33 | 0.24 | 12.2 | ---- | ----- | 2.5 | 0.27 | 800 | Rectilinear |
| | 33 | .49 | 9.0 | 4.4 | 1.69 | 2.8 | 1.13 | 1300 | Zig-zag |
| | 33 | .71 | 7.5 | 4.4 | 1.79 | 2.8 | 2.4 | 1500 | Zig-zag |
| | 49.7 | .19 | 14.0 | ---- | ----- | 2.7 | .26 | 1500 | Rectilinear |
| | 49.7 | .27 | 12.2 | 5.7 | 1.32 | 2.8 | .51 | 900 | Zig-zag |
| | 49.7 | .45 | 9.6 | 5.1 | 1.00 | 2.9 | 1.4 | 1200 | |
| | 49.7 | .49 | 9.8 | 5.0 | 1.17 | 3.3 | 1.7 | 1300 | |
| | 980 | .055 | 26.4 | 51.8 | .064 | 2.7 | .42 | 400 | |
| | 980 | .079 | 23.8 | 57.5 | .068 | 3.1 | .86 | 500 | |
| | 980 | .14 | 18.3 | 23.9 | .142 | 3.3 | 2.7 | 700 | |
| FC-78 | 30 | 0.62 | 5.3 | 5.7 | 0.47 | 4.6 | 6.1 | 1400 | Zig-zag |
| | 45.3 | .62 | 6.4 | 3.9 | .37 | 6.5 | 9.2 | 1700 | Zig-zag |
| | 45.3 | .87 | 6.7 | 5.4 | .70 | 10.2 | 17.5 | 2500 | Helical |
| Trichlorotrifloroethane | 30 | 0.22 | 9.1 | 4.7 | 1.32 | 3.1 | 0.50 | 900 | Zig-zag |
| | 30 | .26 | 7.1 | 4.9 | 1.25 | 2.4 | .73 | 900 | Zig-zag |
| | 30 | .38 | 7.2 | 4.8 | .85 | 3.8 | 1.51 | 1200 | Helical |
| Carbon tetrachloride | 30 | 0.17 | 11.4 | ---- | ----- | 2.7 | 0.21 | 700 | Rectilinear |
| | 30 | .34 | 9.0 | 7.0 | 1.27 | 3.3 | .84 | 1000 | Zig-zag |
| | 30 | .66 | 7.3 | 3.4 | 1.04 | 4.2 | 3.2 | 1700 | Zig-zag |
| 1-Butanol | 980 | 0.03 | 9.7 | ---- | ----- | 0.19 | 0.12 | 19 | Rectilinear |
| | | .04 | 10.4 | ---- | ----- | .29 | .21 | 24 | Rectilinear |
| | | .07 | 21.7 | ---- | ----- | 2.2 | .63 | 86 | Rectilinear |
| | | .11 | 20.2 | 47 | 0.115 | 2.9 | 1.6 | 130 | Zig-zag |
| | | .17 | 19.4 | 47 | .16 | 4.2 | 3.8 | 190 | Zig-zag |

eters (We, $B_o$, and Re) could be determined. A summary of the experimental results is given in table II. The data presented ranged over Reynolds numbers from 19 to 2500.

## Criterion for Unsteady Bubble Motion

The region of stable bubble motion is an important one since many small but observable bubbles fall into this region. Typically, in normal gravity, bubbles less than 0.01

centimeter in radius move in rectilinear paths. Bubbles larger than this (of the order of 0.01 cm in radius) move in helical or zig-zag paths. As the gravity level is reduced, it is known from the results in reference 1 that this rectilinear region extends to much larger radii. The critical radius at which unstable motion occurs in normal gravity appears reasonably well defined. This report examines the corresponding critical radii in low gravity.

If it is indeed true, as normal-gravity theory and experiments indicate, that the beginning of unsteady motion is characterized by a critical Weber number (refs. 2 and 3), it would be expected that the similar critical Weber number relation should hold in low gravity.

The author has observed that, in both normal gravity (ref. 1) and low gravity, instability first occurs in a region where the bubble has become distorted to an ellipsoid. It has been shown (ref. 7) that the terminal velocity of a bubble in this region is given by the relation

$$v = K(\beta a)^{1/4} \tag{5}$$

where $K \cong 1.5$. If the Weber number is constant for the beginning of instability,

$$We = \frac{2v^2 r_{eq}}{\beta} = C \tag{6}$$

the foregoing equations can be solved for the critical radius by eliminating the terminal velocity. The resulting equation is

$$r_{eq} = \frac{C}{2K^2}\left(\frac{\beta}{a}\right)^{1/2} = L\left(\frac{\beta}{a}\right)^{1/2} \tag{7}$$

By substituting Siegel's (ref. 7) $K$ value (1.5) and the critical Weber number found in reference 3 (3.16), $L$ is predicted to be about 0.7. Equation (7) yields that critical radius (above which instability will occur) as a function of liquid properties and the system acceleration. A stability plot of the data presented in table II is shown in figure 8. The solid symbols indicate unsteady motion; the open symbols indicate rectilinear motion. This figure shows that the functional form for the critical equivalent radius is consistent

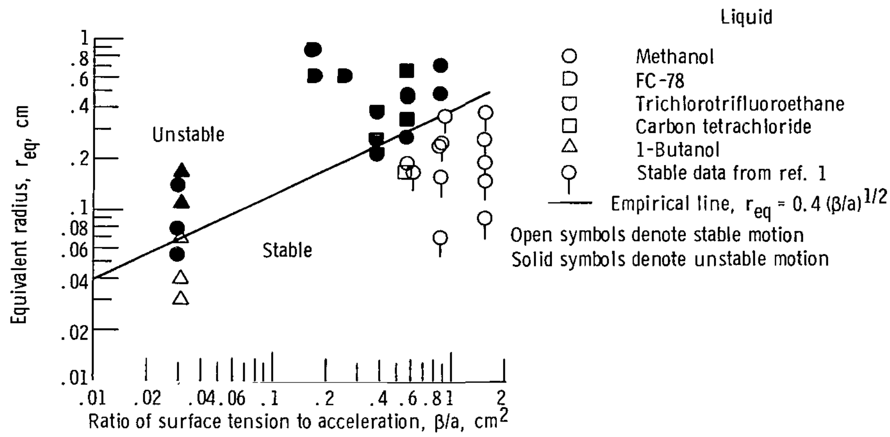


Figure 8. - Types of bubble motion at various gravity levels.

with the assumption of both a critical Weber number and the dependence of the terminal velocity on $(\beta a)^{1/4}$. The empirical line obtained is

$$r_{eq} = 0.4\left(\frac{\beta}{a}\right)^{1/2} \tag{8}$$

Only the constant of proportionality (0.4) in equation (8) differs from the predicted value of 0.7 from references 3 and 7. In normal gravity, Hartunian and Sear's (ref. 3) experimental critical equivalent radii data agree reasonably well with equation (8).

When the Weber number, which is defined as the ratio of hydrodynamic to surface tension forces, is plotted against system acceleration, it is expected that the region of instability should begin at or near a constant Weber number. Indeed, as shown in figure 9, this is the case and the experimental critical Weber number was found to be about

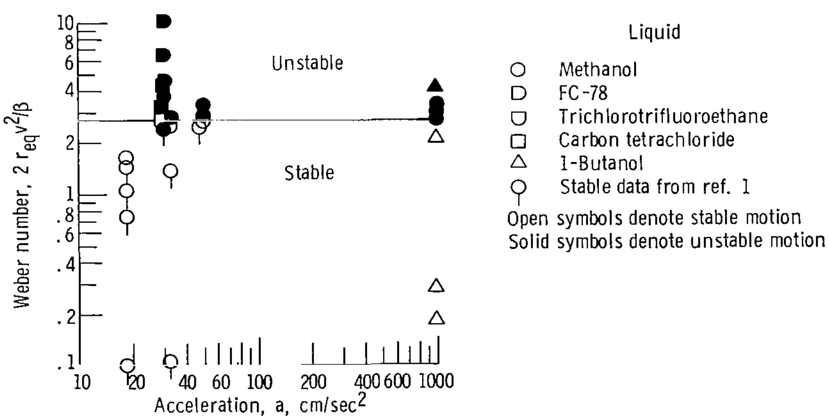


Figure 9. - Dependence of type of bubble motion with Weber number. Critical Weber number, 2.7.

2.7. This value is in fair agreement with Hartunian and Sear's result (critical Weber number of 3.16), though it is somewhat lower. Saffman's result (ref. 2) of We = 1.03 is even lower.

Another interesting result comes to light if equation (8) is reexamined. For this equation to hold, the Bond number of the bubble must be a constant. The Bond number is defined as the ratio of gravitational to surface tension forces. A plot of the Bond numbers of the bubbles in this study against system acceleration is shown in figure 10, where the critical Bond number is 0.64. As a result of the plots in figures 9 and 10, it can be con-

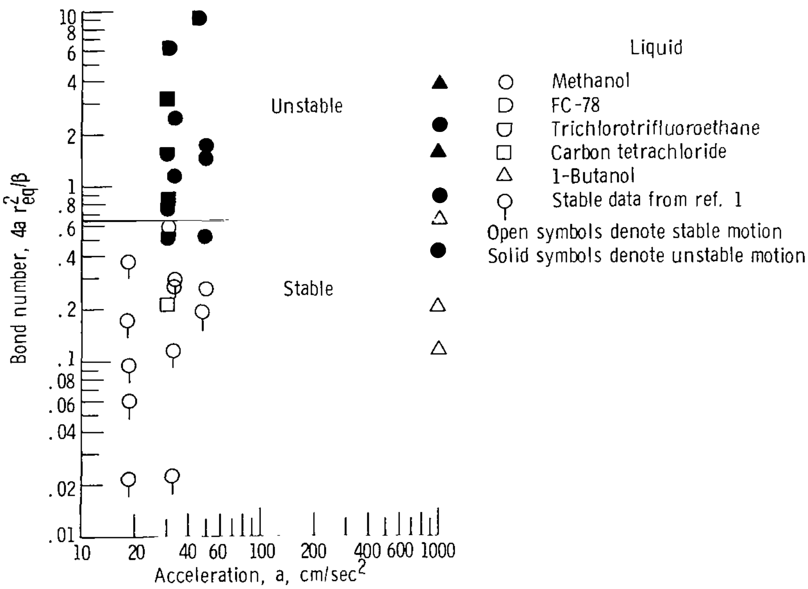


Figure 10. - Dependence of type of bubble motion with Bond number. Critical Bond number, 0.64.

cluded that either the critical Weber number or the critical Bond number criterion is sufficient to predict the onset of unstable bubble motion. What is implied is that for distorted bubbles hydrodynamic forces are a simple function of the acceleration of the system.

## Frequency and Amplitude Data

The frequencies of oscillation of all the bubbles, whether they are traveling in a zigzag or helical path, are presented in figure 11. It is clear from the spread in the data that only trends can be discussed. The frequency of oscillation appears to be directly proportional to the square root of the system acceleration. In normal gravity, Saffman (ref. 2) experimentally found the frequency of oscillation of 30 radians per second for

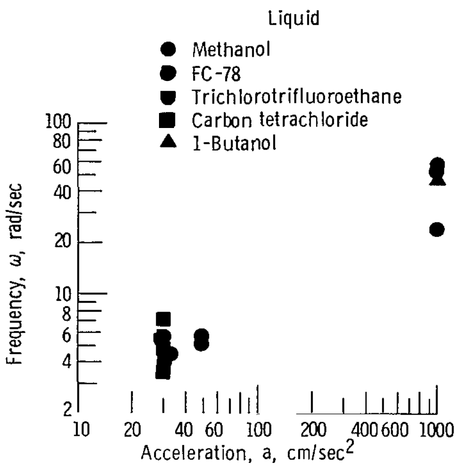


Figure 11. - Frequency of unstable bubble motion at various gravity levels.

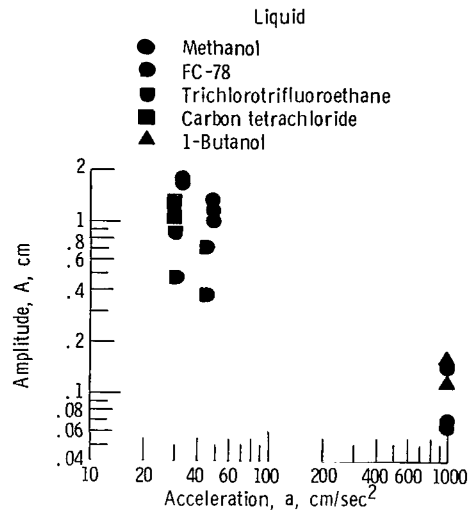


Figure 12. - Amplitude of unstable bubble motion at various gravity levels.

bubbles in water, which agrees reasonably well with the data presented herein.

The amplitude data are presented in figure 12 and show to a good approximation that the amplitude of oscillation is inversely proportional to the square root of the system acceleration. In normal gravity, Saffman (ref. 2) experimentally found the amplitude of oscillation of 0.15 centimeter for bubbles in water, which agrees well with the data of this report. It was also noted that the amplitude of oscillation was dependent on the equivalent radius, as mentioned by Saffman. However, because of scatter in the amplitude data, no mathematical relation was found.

## SUMMARY OF RESULTS

An experimental study was undertaken to determine when unsteady bubble motion would occur in reduced-gravity fields. Measurements of the frequency and amplitude of oscillation, when unsteady motion occurred, were presented. The results were compared with normal-gravity information. The study was conducted at the Lewis Research Center's Zero-Gravity Facility, where gravity levels from 0.03 to 0.05 g were obtained. Bubble radii ranged from 0.17 to 0.87 centimeter. The following results were obtained:

1. The approximate bubble size above which unstable motion will occur for low-viscosity fluids is given by the empirical relation

$$r_{eq} = 0.4\left(\frac{\beta}{a}\right)^{1/2}$$

where $r_{eq}$ is the equivalent radius of the bubble, $\beta$ is the specific surface tension, and $a$ is the acceleration of the system.

2. Both the critical Weber number and critical Bond number above which unstable bubble motion occurs appeared to be constant and independent of the gravity field. That critical Weber number $2r_{eq}v^2/\beta$, where $v$ is the terminal velocity, was about 2.7. The critical Bond number $4r_{eq}^2 a/\beta$ was about 0.64. The implication was that, for distorted bubbles, the hydrodynamic force was a simple function of the acceleration on the system.

3. Unstable bubbles appeared to oscillate with a frequency that was directly proportional to the square root of the system acceleration.

4. The amplitude of oscillation appeared to be inversely proportional to the square root of the system acceleration.

Lewis Research Center,
National Aeronautics and Space Administration,
Cleveland, Ohio, February 13, 1970,
124-08.

## REFERENCES

1. Haggard, John B., Jr.; and Masica, W. J.: Motion of Single Bubbles Under Low Gravitational Conditions. NASA TN D-5462, 1969.

2. Saffman, P. G.: On the Rise of Small Air Bubbles in Water. J. Fluid Mech., vol. 1, pt. 3, Sept. 1956, pp. 249-275.

3. Hartunian, R. A.; and Sears, W. R.: On the Instability of Small Gas Bubbles Moving Uniformly in Various Liquids. J. Fluid Mech., vol. 3, pt. 1, Oct. 1957, pp. 27-47.

4. Coney, Thom A.: Surface Tension, Viscosity, and Density Measurements of Two Fluorocarbon Solvents, FC-43 and FC-78. NASA TM X-1862, 1969.

5. Masica, William J.; and Petrash, Donald A.: Motion of Liquid-Vapor Interface in Response to Imposed Acceleration. NASA TN D-3005, 1965.

6. Uno, Seiji; and Kintner, R. C.: Effect of Wall Proximity on the Rate of Rise of Single Air Bubbles in a Quiescent Liquid. AiChE J., vol. 2, no. 3, Sept. 1956, pp. 420-425.

7. Siegel, Robert: Effects of Reduced Gravity of Heat Transfer. Advances in Heat Transfer. Vol. 4. J. P. Hartnett and T. F. Irvine, Jr., eds., Academic Press, 1967, pp. 190-191.


NASA-Langley, 1970 —— 12 E-5537

*"The aeronautical and space activities of the United States shall be conducted so as to contribute . . . to the expansion of human knowledge of phenomena in the atmosphere and space. The Administration shall provide for the widest practicable and appropriate dissemination of information concerning its activities and the results thereof."*

—NATIONAL AERONAUTICS AND SPACE ACT OF 1958

# NASA SCIENTIFIC AND TECHNICAL PUBLICATIONS

TECHNICAL REPORTS: Scientific and technical information considered important, complete, and a lasting contribution to existing knowledge.

TECHNICAL NOTES: Information less broad in scope but nevertheless of importance as a contribution to existing knowledge.

TECHNICAL MEMORANDUMS: Information receiving limited distribution because of preliminary data, security classification, or other reasons.

CONTRACTOR REPORTS: Scientific and technical information generated under a NASA contract or grant and considered an important contribution to existing knowledge.

TECHNICAL TRANSLATIONS: Information published in a foreign language considered to merit NASA distribution in English.

SPECIAL PUBLICATIONS: Information derived from or of value to NASA activities. Publications include conference proceedings, monographs, data compilations, handbooks, sourcebooks, and special bibliographies.

TECHNOLOGY UTILIZATION PUBLICATIONS: Information on technology used by NASA that may be of particular interest in commercial and other non-aerospace applications. Publications include Tech Briefs, Technology Utilization Reports and Notes, and Technology Surveys.

*Details on the availability of these publications may be obtained from:*

**SCIENTIFIC AND TECHNICAL INFORMATION DIVISION**

**NATIONAL AERONAUTICS AND SPACE ADMINISTRATION**

**Washington, D.C. 20546**